Microtwin Structure in (SN)[X] (Commemoration Issue Dedicated to Professor Natsu Uyeda, on the Occasion of His Retirment)

AUTHOR(S):

Isoda, Seiji; Uemura, Akio; Moriguchi, Sakumi; Ohara, Masayoshi; Katayama, Ken-ichi

CITATION:

Isoda, Seiji ...[et al]. Microtwin Structure in (SN)[X] (Commemoration Issue Dedicated to Professor Natsu Uyeda, on the Occasion of His Retirment). Bulletin of the Institute for Chemical Research, Kyoto University 1989, 66(5): 530-539

ISSUE DATE:

1989-03-15

URL:

http://hdl.handle.net/2433/77277

Bull. Inst. Chem. Res., Kyoto Univ., Vol. 66, No. 5, 1988

Microtwin Structure in $(SN)_x$

Seiji ISODA*, Akio UEMURA*, Sakumi MORIGUCHI*,
Masayoshi OHARA* and Ken-ichi KATAYAMA*

Received September 21, 1988

Microfibrillar structure in $(SN)_x$ was studied by SEM, TEM and STM. The structure is introduced by microtwinning on (100) plane of $(SN)_x$ during the solid state polymerzation from S_2N_2. The lateral size of microfibrils caused by such microtwinning was several nm in width. The very narrow distribution of the lateral crystal sizes can be qualitatively explained by an idea that with increasing lateral crystallite size the lateral growth rate decreases exponentially due to lattice misfit between the S_2N_2 and $(SN)_x$ crystals.

KEY WORDS: Polymeric sulfur nitride/ Microtwin/ Solid state polymerization/ Fibrillation/

I. INTRODUCTION

Since Walatka *et al.*[1] pointed out the possibility that polymeric sulfur nitride $(SN)_x$ is an one-dimensional metallic conductor, many studies by electrical, magnetic, optical and structural methods have been carried out to investigate its metallic and superconducting[2] properties. The electrical properties are now considered to be characteristic of an anisotropic three-dimensional metal rather than a quasi-one-dimensional one.

$(SN)_x$ is prepared by the thermal polymerization (solid state polymerization) of vapour-phase-grown crystals of dimer S_2N_2[3]. Usually $(SN)_x$ is obtained in a defect-rich crystalline state with a size of mm, all over which microfibrillar structures of 5–10 nm width are formed. These microfibrous structures are considered to be resulted from the solid state polymerization proceeding through microtwinning process[3].

In order to explain the Meissner effect and the susceptibility at the superconducting transition region in $(SN)_x$, the bundle model[4] and the weakly coupled filamentary superconductor model[5] were proposed from the microstructural point of view. In order to improve electrical properties, $(SN)_x$ was doped with bromine or iodine atoms and it is believed that the dopants are intercalated among polymer chains to form a sort of super-lattice[6]. In this case the dopants were found to invade preferentially along the chain axis[7]. Therefore not only the chain orientation but also the presence of this microfibrous texture influence strongly most of macroscopic properties of $(SN)_x$ crystals. A detailed investigation of the structure is essential for the understanding of their properties.

* 磯田正二，植村明夫，森口作美，小原正義，片山健一：Laboratory of Polymer Crystals, Institute for Chemical Research, Kyoto University.

II. EXPERIMENTAL

$(SN)_x$ crystals were grown by the spontaneous solid state polymerization of single crystals of S_2N_2, which was produced beforehand by the thermal decomposition of S_4N_4 passing through a heated silver wool[1]. The $(SN)_x$ specimen was evacuated for 1 day in order to eliminate any traces of S_2N_2 before further experiments. For transmission electron microscopic (TEM) experiments the $(SN)_x$ crystal was crushed into fine pieces in liquid nitrogen to prevent the crystal from severe deformation. Fine fibrous specimens thus prepared were examined with an electron microscope (JEM-200CS) operated at 200 kV. The surface of as-prepared $(SN)_x$ crystal was examined with scanning electron microscope (SEM), Hitachi S-310, and scanning tunnelling microscope (STM), Nano Scope II.

The crystal structure of $(SN)_x$ investigated is the monoclinic form; $a=0.4153$ nm, $b=0.4439$ nm (the chain axis), $c=0.7637$ nm and $\beta=109.7°$ [8].

III. RESULTS AND DISCUSSION

By SEM observation, $(SN)_x$ has a fibrous morphology extended largely along in the chain axis and the width of the fibril is of some hundreds nm as shown in Fig. 1. Moreover in the fibrils, finer microfibrils (narrower than 10 nm in the direction normal to the chain axis) are observed by TEM as shown in a dark-field image of Fig. 2-a taken with $h0l$ reflections. Such a microfibrillar structure is considered to come from the repitition of microtwinning on the (100) plane of $(SN)_x$ during the solid state polymerization[3]. Another twin mode was proposed by Stejny *et al.*[9], that is, a twin on $(\bar{1}01)$ plane, from the fact that 200 and $\bar{1}02$ reflections occasionally appeared together in a selected area electron diffraction pattern.

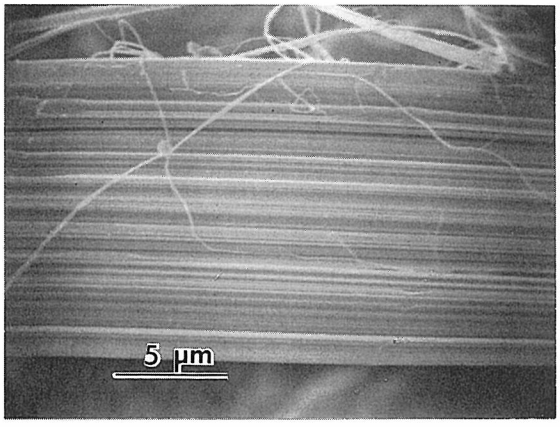

Fig. 1. Fibrillar texture of some hundreds nm width observed in SEM image from $(SN)_x$ surface. The chain axis is horizontal.

Further TEM observation on the finer microfibrils was carried out to take the lattice image of $(SN)_x$. Figure 3 shows an example of lattice image in the $(SN)_x$

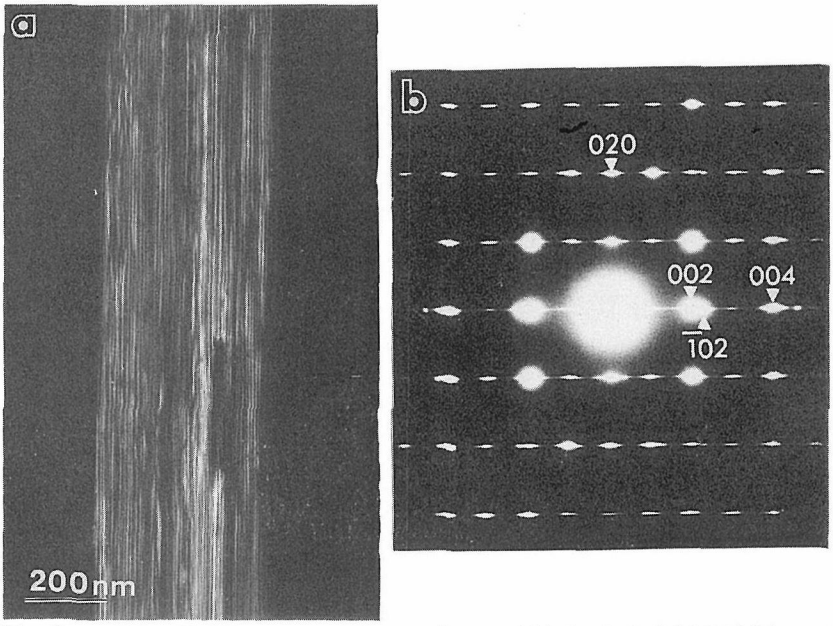

Fig. 2. a. Microfibrillar texture of several nm width in dark field TEM image obtained by using $h0l$ reflections. The chain axis is vertical. b. Typical selected area electron diffraction pattern, where the 002 and $\bar{1}02$ reflections are frequently observed together.

fiber, where the chain direction (the *b*-axis) is shown by an arrow. Bands are seen, in which one kind of lattice fringes (corresponding to 002 spacing of 0.36 nm) are running along the chain direction. The band width is several nm, corresponding to that of the bright domains in the dark field image in Fig. 2-a. Usually, we could not find two kinds of lattice fringes, (002) and ($\bar{1}02$), in a same area of such highly magnified images, while their reflections are simulteneously observed in the selected area electron diffraction pattern taken by normal way. Another lattice fringes corresponding to (012), spacing of 0.28 nm, is also observed partly in the image.

Figure 4 shows the relation in the reciprocal space between twinned crystals on (100) plane of $(SN)_x$. The 002 and $\bar{1}02$ reciprocal lattice points appear near in the same direction, but not exactly on the same line. When the orientation of microfibrillar crystallites varies a little from place to place, the both reflections are expected to appear together in a selected area electron diffraction pattern, because a relatively larger area is irradiated by electron beam. In a highly magnified image, however, lattice images only from a smaller area are photographed, so that the change of orientation of crystallites can be identified locally in a very small scale, when the Bragg reflections are excited. As only 002 lattice fringes are recorded in this case, one type of twinned crystals is observed as the band.

Such microtwin structure depends largely on conditions in preparation. For example, Nakada[10] has shown an improved method to prepare a larger single crystal of $(SN)_x$ by controlling the number of nuclei to grow. For his specimen,

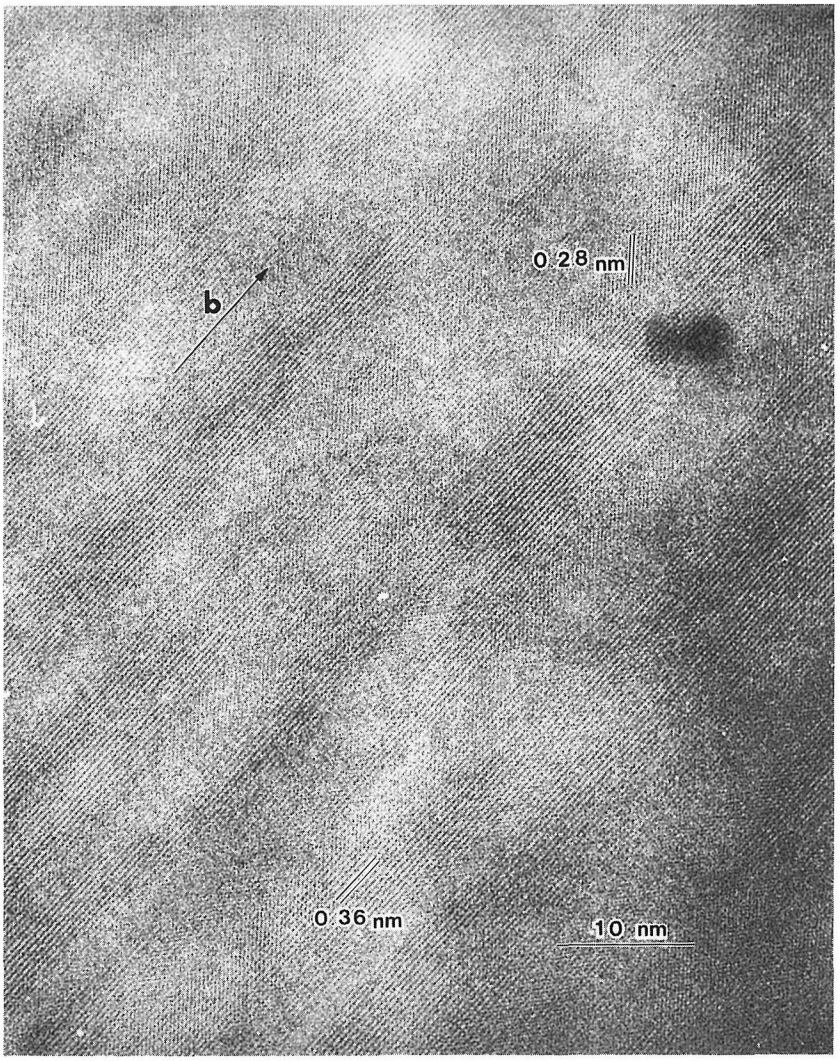

Fig. 3. Lattice images showing microtwin structure. Lattice fringes correspondeng to (002) spacing of 0.36 nm and to (012) spacing of 0.28 nm are observed, and in particular the 002 lattice fringes are observed in domains narrow in the lateral direction and long in the chain axis.

002 reflection appeares in some cases without being accompanied with $\bar{1}02$ reflection even in selected area electron diffraction. This means that microtwinning less frequently occurs by his method.

Baughman *et al.*[3] have already reported the favorable (100) twin in the consideration of solid state polymerization as shown in Figs. 5 and 6. The S_2N_2 dimers in the single crystal are polymerized by the ring opening reaction and are crystallized to form $(SN)_x$ crystals whose chain axis coincides to the *a*-axis of the dimer crystal. The lattice matching between the S_2N_2 dimer and the $(SN)_x$ crystals is well in the case of (100) twinning shown in A of Fig. 6. The misfit is 1.3% for

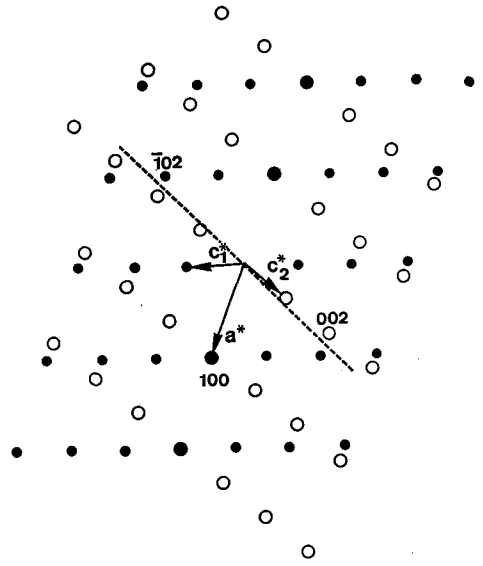

Fig. 4. The relation of the reciprocal lattices (denoted by open and closed circles) of tiwinned crystals. The 002 and $\bar{1}02$ reflections are expected to appear in nearly the same incidence of electrons.

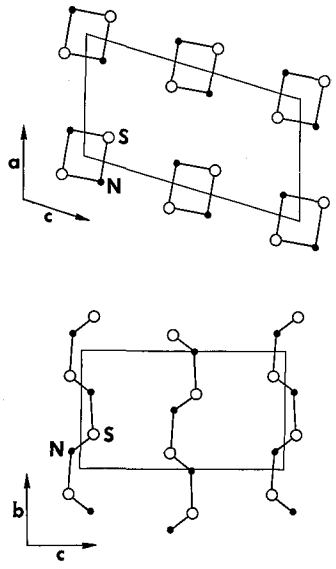

Fig. 5. A model for the solid state polymerization of $(SN)_x$ from S_2N_2 dimer single crystal through ring opening reaction, described by Baughman *et al.*[3].

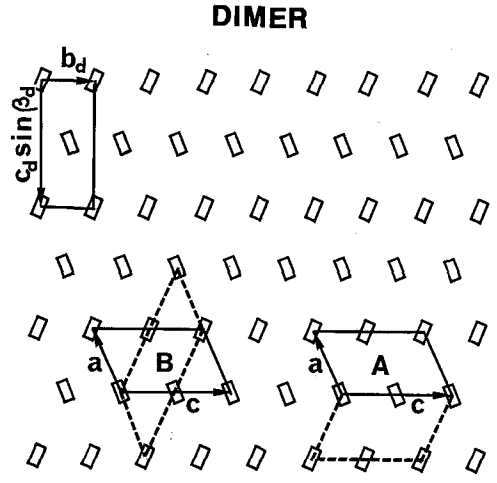

Fig. 6. Schematic drawing showing how the twin of $(SN)_x$ occurs from the dimer crystal. As shown in Fig. 5, the *a*-axis of dimer transforms directly to the chain axis (the *b*-axis) of $(SN)_x$. A; twin on (100) of $(SN)_x$, B; twin on $(\bar{1}01)$ of $(SN)_x$. Here the B-type twin is energetically unfavourable, if there is no large change in positions of dimer and the polymer molecules during the polymerization.

the *c*-axis, 7.7% for the *a*-axis and −1.0% for the chain axis of $(SN)_x$. Since there is no energetic difference between polymerizations taking place in dimer crystals in the twin relation (two unit cells in the twin relation are shown with full and dotted lines in A of Fig. 6, respectively), the $(SN)_x$ crystallites with respective orientations are found with equal probability in the resulted polymer crystal retaining the twin relation one another. Another microtwinning mode, twinning on $(\bar{1}01)$ plane proposed by Stejny *et al.*[9] shown in B of the figure, is not energetically favourable, but still expected. When the polymerization continues on the $(\bar{1}01)$ plane by keeping the twin relation between the resulted polymer crystallites in the dimer crystal, the lattice misfit between both is higher. In this case the misfit values are the same for one of twinned crystals (shown by full lines) with the A mode, but higher for the other (dotted unit cell), that is, 9.3% for the *c*-axis and −17.1% for the *a*-axis. Such twinning on $(\bar{1}01)$ was also observed in our experiment, although seldom. In our specimens, the (100) twin is predominant.

Next let us consider the crystallization process in $(SN)_x$ that realizes the observed microfibrillar structure. Some researchers have reported the regular (or periodic) stacking of band structures by electron microscopy, fov example, by the small angle electron diffraction method[11] and by analysis of intensity modulation in streaked *hkl* electron reflections[9]. But for macroscopic specimens, such periodic nature was not detected by X-ray analysis and therefore the periodic stacking might be a very local phenomenon, if it would exist. For our specimens we did not find any signs of indicating the periodically banded structure. Nevertheless, the distribution of the band width seems to be so narrow that each band has roughly the same lateral size, as shown in dark field image (Fig. 2-a) and lattice image in Fig. 3. A similar fiber formation was described by Wegner *et al.*[12] for poly (oxymethylene) prepared by the solid state polymerization of 1, 3, 5-trioxane. They considered that the polymer grows rapidly in the chain direction, but the crystal growth soon stops in the lateral directions, because the chains become out of register due to lattice misfit between the monomer and the poly(oxymethylene) crystals.

According to this idea, we present a simple model to explain the microfibrillar structures with roughly regular band width. Here, for simplicity, the anisotropy in the *ac*-plane is ignored and we treat the problem in two-dimension: along the chain axis and in the normal direction to the chain. Whether the microtwin on (100) or on $(\bar{1}01)$ occurs, the lateral misfit is worse than that along the chain direction. The S_2N_2 dimers are polymerized easily into the $(SN)_x$ along the chain axis. As poly merization proceeds, the $(SN)_x$ crystal grows rapidly and linearly in the direction parallel to the chain axis;

$$dR_{\parallel}/dt = k_{\parallel} \text{ and } k_{\parallel} = \text{constant},$$

but in the lateral direction the crystal grows following the next equation,

$$dR_{\perp}/dt = k_{\perp} \text{ and } k_{\perp} = k_{\perp}^{0} \exp(-R_{\perp}/R_{\perp}^{0}),$$

where $R_{\parallel}$ and $R_{\perp}$ are the crystal size at time t in the directions parallel and perpendicular to the chain axis, respectively, $k_{\parallel}$ and $k_{\perp}$ the growth rates ($k_{\parallel} \gg k_{\perp}$)

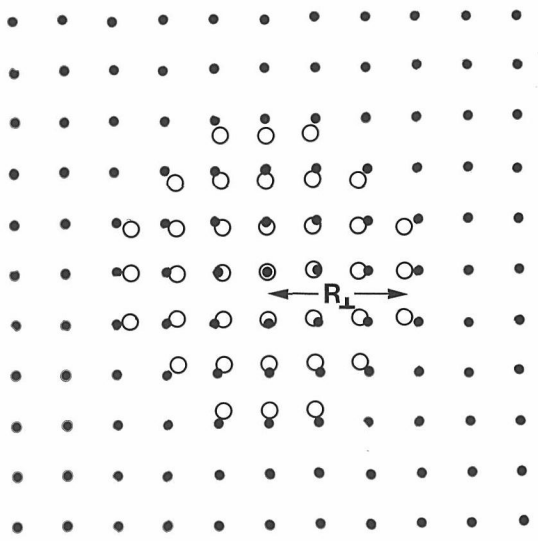

Fig. 7. Schematic presentation of lattice misfit between the dimer (●) and the polymer (○) as a projection along the chain axis of the polymer. When polymer crystal grows to the distance of $R_{\perp}$, coherent crystallization is no longer able to continue due to the large positional misfit.

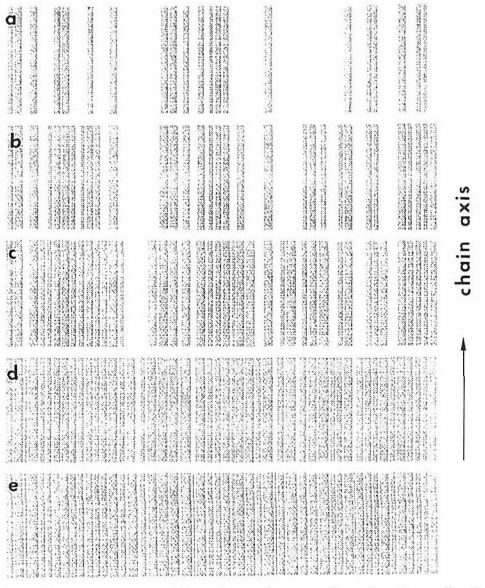

Fig. 8. Band structure simulated on the basis of the highly anisotropic growth in the case of $R_{\perp}{}^{0}=1$. Models a-e show the growth of band structure with time.

for corresponding directions, and $k_\perp{}^0$ and $R_\perp{}^0$ the constants. In the last equation the lateral growth rate $k_\perp$ are assumed to decrease exponentially with increasing the lateral size $R_\perp$, because molecular positions of polymers formed at the boundary between the polymer and the dimer crystals are more and more displaced from the registered positions for the polymer crystal lattice as the polymerization and

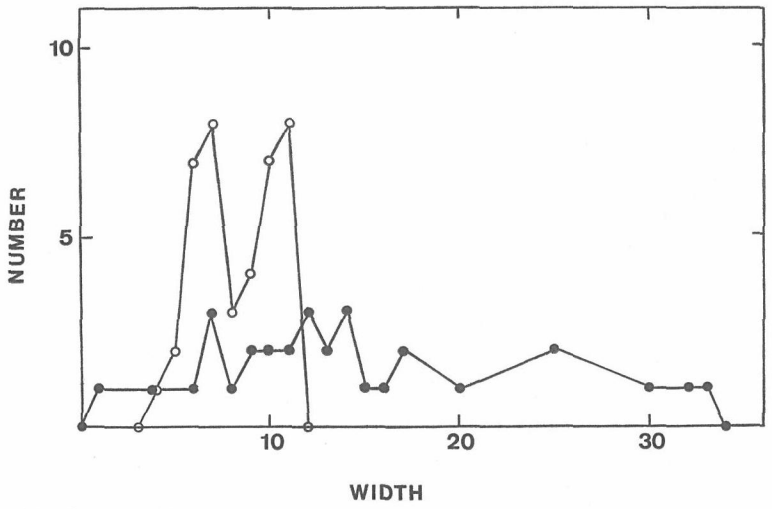

Fig. 9. Distribution of crystal widths counted in the simulated band structures at the final state for $R_\perp{}^0=1$ (○) and $R_\perp{}^0=20$ (●).

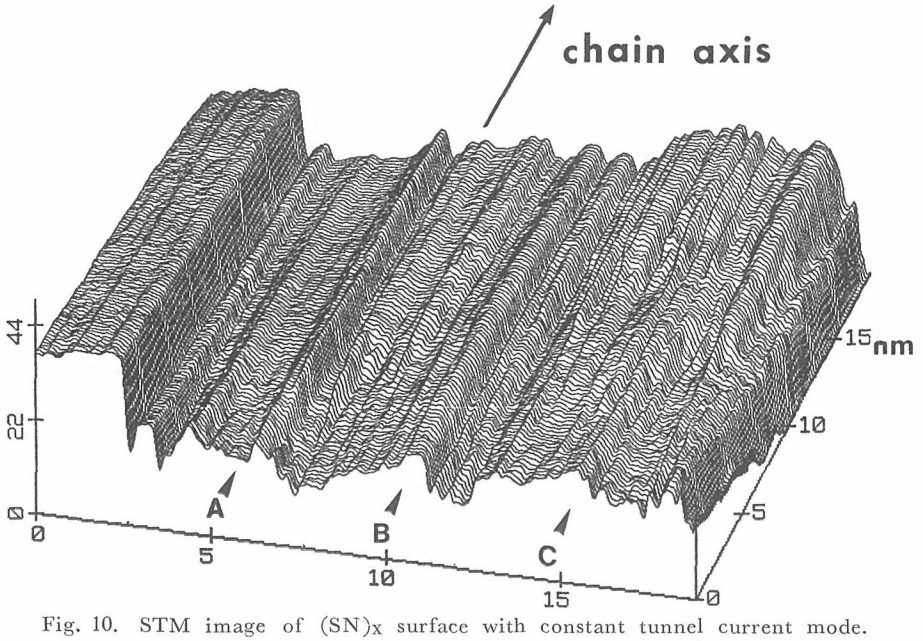

Fig. 10. STM image of $(SN)_x$ surface with constant tunnel current mode. Anisotropic feature is observed and barrel vaults (shown by A, B and C) are found, which correspond to the band structure observed by TEM.

the crystallization proceed (Fig. 7).

A simulated time sequence of crystal growth using above equations is shown in Fig. 8, where each black rectangle is one microfibrillar crystallite grown from nuclei randomly produced in space and time. The vertical in the figure corresponds to the chain direction. As expected from the growth equation for the lateral direction, the crystal growth is decreased in nearly the same width shown in Fig. 8-e. The distribution of the band widths is plotted in Fig. 9 for two $R_{\perp}^{0}$ values; open circles for the case of $R_{\perp}^{0}=1$ and closed ones for $R_{\perp}^{0}=20$. From the crystallization mechanism mentioned above, it is no wonder that the narrower distribution of band width is attained for a smaller $R_{\perp}^{0}$ value, because it is difficult to grow over a threshold value of the width.

Such a microtwin structure on the surface could not be observed by SEM, but possibly by STM because of its higher resolution. Figure 10 shows a surface structure of microtwinned crystals, obtained by STM. Although the surface is certainly contaminated in air, a structure like a range of mountains is found along the chain axis and moreover barrel vaults with the width of about 5 nm shown by A, B and C in the figure. These vaults are supposed to correspond to the microtwin structure and the twinned crystals seem to grow in a form of cylinder. It is not easy to interprete the STM image of $(SN)_x$ in atomic scale due to the surface roughness and the highly anisotropic Fermi surface. Detailed analysis of the STM atomic image is under way.

IV. CONCLUSIONS

1. Microtwin structure was observed in $(SN)_x$ by TEM and STM, and the twinning on (100) is most probable from electron microscopy and lattice matching consideration.

2. The banded structure due to the microfibrillation is originated from the high anisotropy of crystal growth rates and the regular alignment of the band structures can be explained by the concept that the lateral growth rate is proportional to exp $(-R_{\perp}/R_{\perp}^{0})$.

ACKNOWLEDGEMENTS

The authors express their thanks to Toyo Technica for allowance to use Nano Scope II. We are also grateful to Prof. K. Kawaguchi for many discussions.

REFERENCES

(1) V.V. Walatka, M.M. Labes and J.H. Perlstein, *Phys. Rev. Lett.*, **31**, 1139 (1973).
(2) R.L. Greene, G.B. Street and L.J. Suter, *Phys. Rev. Lett.* **34**, 577 (1975).
(3) R.H. Baughman, R.R. Chance and M.J. Cohen, *J. Chem. Phys.* **64**, 1869 (1976).
(4) R.H. Dee, D.H. Dollard, B.G. Turrell and J.F. Carolan, *Solid State Commun.* **24**, 469 (1977).
(5) Y. Oda, H. Takenaka, H. Nagano and I. Nakada, *Solid State Commun.*, **32**, 659 (1979).
(6) S. Isoda, A. Kawaguchi, A. Uemura and K. Katayama, *Jpn. J. Appl. Phys.*, **24**, L341 (1985).
(7) A. Kawaguchi, S. Isoda, J. Petermann and K. Katayama, *Colloid & Polym. Sci.*, **263**, 631 (1985).
(8) M.J. Cohen, A.F. Garito, A.J. Heeger, A.G. MacDiarmid, C.M. Mikulski, M.S. Saran and

J. Kleppinger, *J. Amer. Chem. Soc.*, **98**, 3844 (1976).
(9) J. Stejny, J. Dlugosz and A. Keller, *J. Mater. Sci.*, **14**, 1291 (1979).
(10) I. Nakada, *J. Cryst. Growth*, **55**, 447 (1981).
(11) J.M. Schultz, J. Bentley, R.W. Hendricks, L.S. Lin and J. Petermann, *J. Appl. Phys.*, **52**, 5389 (1981).
(12) G. Wegner, E.W. Fisher and A.M. Escalona, *Makromol. Chem. Suppl.*, **1**, 521 (1975).